Apical and Basal Orthodromic Population Spikes in Hippocampal CA1 In Vivo Show Different Origins and Patterns of Propagation

FABIAN KLOOSTERMAN, PASCAL PELOQUIN, AND L. STAN LEUNG
Department of Physiology and Clinical Neurological Sciences, University of Western Ontario, London, Ontario N6A 5A5, Canada

Received 15 December 2000; accepted in final form 16 May 2001

Kloosterman, Fabian, Pascal Peloquin, and L. Stan Leung. Apical and basal orthodromic population spikes in hippocampal CA1 in vivo show different origins and patterns of propagation. *J Neurophysiol* 86: 2435–2444, 2001. There is controversy concerning whether orthodromic action potentials originate from the apical or basal dendrites of CA1 pyramidal cells in vivo. The participation of the dendrites in the initialization and propagation of population spikes in CA1 of urethan-anesthetized rats in vivo was studied using simultaneously recorded field potentials and current source density (CSD) analysis. CSD analysis revealed that the antidromic population spike, evoked by stimulation of the alveus, invaded in succession, the axon initial segment (stratum oriens), cell body and ~200 μm of the proximal apical dendrites. Excitation of the basal dendrites of CA1, following stimulation of CA3 stratum oriens, evoked an orthodromic spike that started near the cell body or initial segment and then propagated ~200 μm into the proximal apical dendrites. In contrast, the population spike that followed excitation of the apical dendrites of CA1 initiated at the proximal apical dendrites, 50–100 μm distal to the cell body layer, and then propagated centripetally to the cell body and the proximal basal dendrites. A late apical dendritic spike may arise in the mid-apical dendrites (250–300 μm from the cell layer) and propagated distally. The origin or the pattern of propagation of each population spike type was similar for near-threshold to supramaximal stimulus intensities. In summary, population spikes following apical dendritic and basal dendritic excitation in vivo appeared to originate from different locations. Apical dendritic excitation evoked a population spike that initiated in the proximal apical dendrites while basal dendritic excitation evoked a spike that started near the initial segment or cell body. An original finding of this study is the propagation of the population spike from basal to apical dendrites in vivo or vice versa. This backpropagation from one dendritic tree to the other may play an important role in the synaptic plasticity among a network of CA3 to CA1 neurons.

INTRODUCTION

Recent studies revealed that the dendrites of neurons are not passive structures that merely provide electrotonic spread of postsynaptic potentials. Instead, the dendrites may generate spikes or otherwise amplify postsynaptic signals by means of voltage-sensitive Na^+ and Ca^{2+} channels (Buzsáki et al. 1996; Magee and Johnston 1995a,b; Spencer and Kandel 1968; Spruston et al. 1995; Wong et al. 1979). A model of dendritic function that emerged from in vitro patch-clamp studies is that during weak orthodromic activation, a cortical pyramidal cell fires near the cell body and this spike backpropagates down the dendrites (Jaffe et al. 1992; Spruston et al. 1995).

Conflicting results showed that spikes start at the apical dendrites of hippocampal CA1 pyramidal cells in vivo. Field potential profiles suggested that orthodromic spikes started at the proximal apical dendrites of CA1 pyramidal cells in anesthetized rabbits and cats, following excitation of the apical dendrites by the Schaffer collaterals (Andersen and Lomo 1966; Fujita and Sakata 1962). Current source density (CSD) analysis in anesthetized rats confirmed that the orthodromic population spike started at the proximal apical dendrites of CA1 (Herreras 1990). Apical dendritic spikes were found using extracellular recordings in vitro (Taube and Schwartzkroin 1988; Turner et al. 1989; Vida et al. 1995), but the predominant view is that an apical dendritic spike was only generated by high-intensity stimulation of the Schaffer collaterals (Golding and Spruston 1998; Turner et al. 1991, 1993). Furthermore, CSD studies of orthodromic population spikes in CA1 in vitro consistently showed that spikes originated near the cell body layer and not at the dendrites (Miyakawa and Kato 1986; Richardson et al. 1987).

It is possible that the afferent stimulus intensity was a confounding variable in the origin of the population spike, but this issue has not been investigated. The in vivo study of Herreras (1990) relied mostly on supramaximal stimulation and the in vitro studies (Miyakawa and Kato 1986; Richardson et al. 1987) likely used high stimulus intensities as well, although it is difficult to compare the stimulus intensities in vivo and in vitro. Richardson et al. (1987) concluded that the orthodromic population spike originated near the cell layer in vitro, irrespective of whether the basal or apical dendrites were excited. The origin of basal dendritic spikes in vivo has not been studied. Thus our objective was to study orthodromic population spikes in CA1 of urethan-anesthetized rats in vivo, following basal or apical dendritic excitation of near-threshold to supramaximal stimulus intensities.

In distinction to previous studies, we analyzed CSDs derived from simultaneous recordings at multiple sites. The alternate technique of deriving CSDs from sequentially acquired evoked potentials assumes that the responses are stationary in time, which may be violated by the notorious variability of orthodromic spikes. In theory, a potential field is generated instan-

Address for reprint requests: L. S. Leung, Dept. of Clinical Neurological Sciences, University Campus, LHSC, University of Western Ontario, London, Ontario N6A 5A5, Canada (E-mail: sleung@uwo.ca).

The costs of publication of this article were defrayed in part by the payment of page charges. The article must therefore be hereby marked "*advertisement*" in accordance with 18 U.S.C. Section 1734 solely to indicate this fact.

taneously (Plonsey 1969) and extracellular potentials at different sites should be acquired simultaneously. We used silicon probes fabricated with precise interelectrode distances (Bement et al. 1986; Ylinen et al. 1995); the accurate spatial interval reduces the error in the CSD estimates.

We found different origins and patterns of propagation for the orthodromic population spike following apical dendritic excitation, as compared with that following basal dendritic excitation or that following antidromic stimulation. Part of the study was presented as an abstract (Leung et al. 2000).

METHODS

Rats (220–450 g) were anesthetized with urethan (1.2–1.5 g/kg ip). The recording probes were positioned in CA1 area at P3.6–4.5, L2.4–3 (with respect to bregma). Stimulating electrodes were placed in *1*) alveus in CA1 at 0.5–1.5 mm posterior and slightly lateral to the recording site; *2*) stratum oriens of CA3a or CA3b, at P3.2, L3.3, 2.9–3.1 mm below the skull surface, to activate the basal dendritic synapses of CA1; and *3*) stratum radiatum of CA3b to activate the apical dendritic synapses of CA1. Stimulation rate was <0.1 Hz.

Silicon recording probes were provided by the National Institutes of Health Center of Neural Communication Technology, University of Michigan. The typical probe used had 16 recording sites spaced 50 μm apart on a vertical shank ("16 channel"). Preliminary data were collected in 12 rats using a 16-channel probe of 100-μm interval; these data are consistent with the conclusions of the present study but are not included in RESULTS. Another probe had two shanks separated by 300 μm and 6 recording sites at 25-μm intervals on each shank ("2 × 6 channel"). In some experiments, the 2 × 6–channel probe was moved 100 μm deeper after a set of recordings, to obtain more depth coverage. The stability of the response was determined by superposition of records at the same absolute depth after repositioning. The signals were amplified 200–1,000 times by preamplifier and amplifier and passed through a high-pass filter with 0.08-Hz corner frequency. Sixteen sample-and-hold circuits maintained the simultaneity of the signals during digitization by a 16-bit A/D converter at 20–40 kHz. Single or average ($n = 4$) sweeps were stored by a custom program. One-dimensional CSD(z, t) as a function of depth z and time t was calculated by a second-order differencing formula (Freeman and Nicholson 1975; Leung 1990)

$$\mathrm{CSD}(z, t) = \sigma[2\Phi(z, t) - \Phi(z + N\Delta z, t) - \Phi(z - N\Delta z, t)]/(N\Delta z)^2 \quad (1)$$

where $\Phi(z, t)$ is the potential at depth z and time t, and Δz is the spacing between adjacent electrodes on the silicon probe, i.e., 25 μm for the 2 × 6 channel probe and 50 μm for the 16-channel probe. Unless otherwise noted, $n = 2$ was used in the equation to spatially smooth the CSDs (Freeman and Nicholson 1975; Leung 1990), the conductivity σ was assumed to be constant, and the CSDs are reported in units of V/mm^2. Analysis of the potential profiles was also made with the values of nonuniform conductivity $\sigma(z)$ as determined by Holsheimer (1987, Fig. 3*B*), using the cell layer as the point of match up. The formula used for nonuniform conductivity ($n = 1$) was

$$\mathrm{CSD}(z, t) = \{\sigma(z)[\Phi(z, t) - \Phi(z - \Delta z, t)] - \sigma(z + \Delta z)[\Phi(z + \Delta z, t) - \Phi(z, t)]\}/(\Delta z)^2 \quad (2)$$

After the experiment, the site of each stimulating electrode was lesioned by passing 0.5- to 1-mA current for 1- to 2-s duration. In experiments using the 16-channel silicon probe, the most ventral electrode of the probe was marked by a lesion, using a current of 50 μA for 3- to 15-s duration. The rat brain was removed after intracardial perfusion with phosphate-buffered saline and 4% Formalin and was later sliced into 40-μm-thick coronal sections. The lesioned sites and the recording track were identified in slide-mounted sections stained with thionin.

CSD events related to the population spike were isolated by subtracting the CSDs associated with the field excitatory postsynaptic potentials (fEPSPs). At a high stimulus intensity, a set of CSD1(z, t) was assumed to consist of a population spike superimposed on the fEPSP. At each depth, a template for the fEPSP was provided by the response CSD2(z, t) evoked by a low stimulus intensity below the population spike threshold. A new response CSD3(z, t) = Amp * CSD2($z, t - \Delta t$), was the fEPSP template scaled by an amplification factor (Amp) and time-shifted by Δt. The time shift was necessary to optimize responses across a range of stimulus intensity. Intracellular EPSPs recorded in vitro showed an earlier onset latency for high than low stimulus intensity (data not shown). Different values for Amp and Δt were iterated by a microcomputer to minimize the sum square error, Σ [CSD3(z, t) − CSD1(z, t)]^2, over all channels and for the duration of the rising phase of the fEPSPs before the spike.

RESULTS

The data from 25 rats were reported in this study: 22 using the 50-μm 16-channel probe and 3 using the 2 × 6–channel probe. Small dye injections (data not shown, but see technique in Leung et al. 1995) at the depth of the maximal sink of the antidromic population spike was found within the CA1 pyramidal cell layer, confirming previous results (Leung 1979b; Lopez-Aguado et al. 2000). Thus the maximal antidromic spike sink was assumed to mark the middle of the pyramidal cell layer. The error of this assumption was estimated at ~25 μm, half the width of the cell layer. A lesion made by the deepest electrode of the silicon probe (not shown) was also consistent with the cell layer depth estimate. The pyramidal cell layer was assigned a depth of 0 μm, and "positive" depth was defined to be toward apical dendrites.

CSD profiles of an antidromic population spike

An antidromic population spike was evoked by stimulation of the alveus, with a threshold of about 29 ± 4 μA (mean ± SE, $n = 21$ rats). Alvear stimulation first activated a compound action potential generated by the axonal fibers in the alveus, many of which were axon collaterals of CA1 pyramidal cells (Leung 1979a). Depth recordings of the field potentials showed a fast negative transient traveling from the alveus to the stratum oriens and then the cell layer (Fig. 1*A*) (Leung 1979a,b; Richardson et al. 1987).

CSD analysis of the depth potentials revealed an early but small sink in stratum oriens, which was interpreted as a current sink at the axon initial segments (IS at −100 μm in Figs. 1*C* and 2*A*). The IS sink was followed by a much larger somatic spike sink (SS) at the cell body layer (0 μm). After a short delay, the cell body sink was followed by an apical dendritic sink (AS at 100–150 μm in Figs. 1*C* and 2*A*). Depth profiles of the CSD at fixed time instants show that the first detectable dipole field at ~1 ms latency was a sink maximal at −100 μm (Fig. 3*A*) accompanied by sources at the proximal apical dendrites (50–150 μm). At 1.4-s latency, the peak sink invaded the cell layer (0 μm) before propagating into the proximal apical dendrites (2- and 2.2-ms latency in Fig. 3*A*).

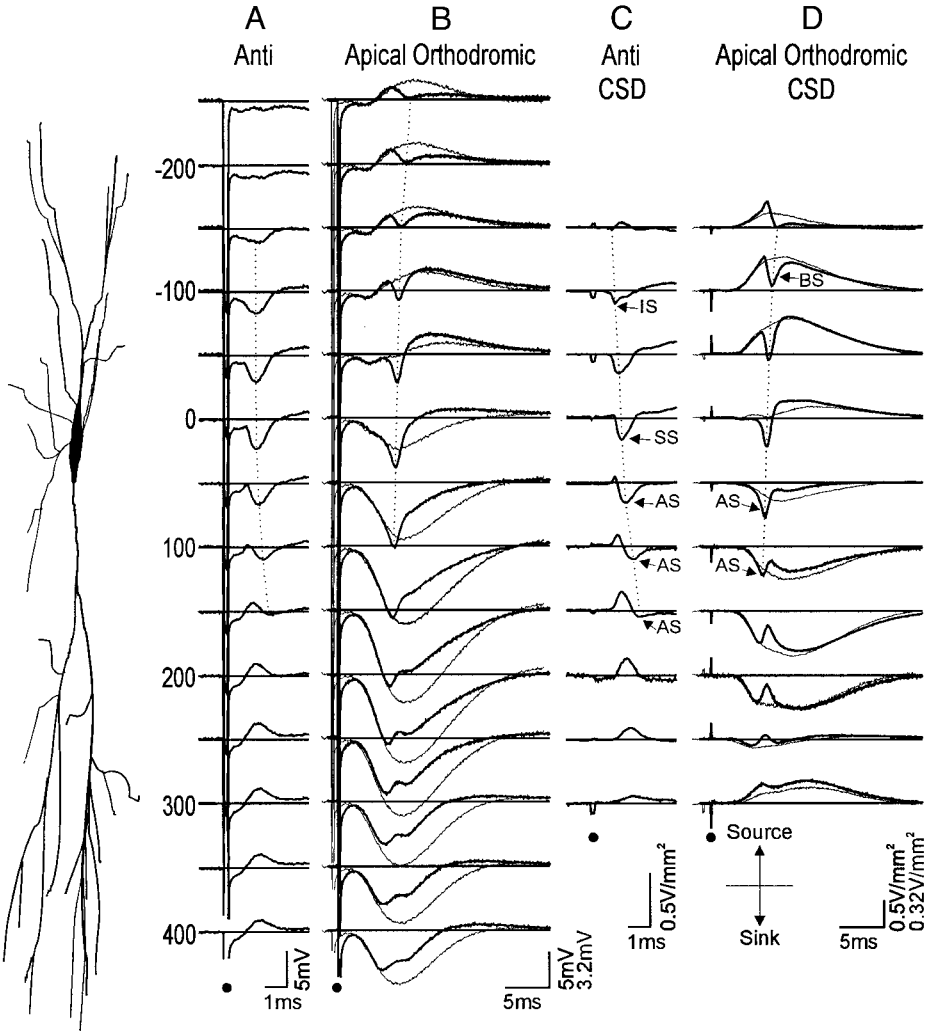

FIG. 1. Average evoked potentials (AEPs; *A* and *B*) and current source density (CSD; *C* and *D*) transients in CA1 of 1 rat (*PBP40*) following antidromic (Anti; *A* and *C*) or apical-dendritic orthodromic excitation (*B* and *D*). Potentials were recorded simultaneously by a 16-electrode silicon probe with 50-μm interval between electrodes. Depths are indicated by the schematic CA1 pyramidal cell drawn and by the distance (in μm) away from the cell body layer (+ toward the apical dendrites). Spike peaks are linked by a dotted line, indicating propagation direction. *A*: AEPs (average of 4 sweeps) following stimulation of the alveus near subiculum at 40 μA (2 times threshold). Artifacts indicated by the solid circle underneath. *B*: orthodromic apical dendritic responses resulted from low- (60 μA; light traces) and high-intensity (dark traces, 240 μA) stimulation of CA3. The low-intensity responses were amplified and time advanced to fit the rising phase of the responses following high-intensity stimulation. *C*: CSD profiles derived from the AEPs shown in *A*. The antidromic spike sink progressively invaded the initial segment (IS), soma (SS), and apical dendrites (AS). *D*: CSD profiles derived from AEPs shown in *B*, following apical dendritic excitation. Apical dendritic excitation generated an apical dendritic spike (AS) at 100 μm that propagated into the cell bodies and then basal dendrites (BS = basal dendritic spike). Dark traces were derived from the high-intensity (240 μA) responses, overlaid on the light traces (60 μA) that were amplified and time-shifted to simulate the rising excitatory postsynaptic potential (EPSP) of the high-intensity responses.

Patterns of origin and propagation of apical orthodromic population spike

Apical dendritic excitation of CA1 was evoked by stimulation of CA3b stratum radiatum, with a stimulus threshold of 20 ± 1.6 μA ($n = 17$). The field potential was negative at the apical dendrites and positive at the basal dendrites (Fig. 1*B*). CSDs showed a maximal fEPSP sink at the apical dendrites (50–200 μm) and sources elsewhere in CA1 (Fig. 1*D*). The threshold for evoking a population spike at the cell body layer was 105 ± 13 μA ($n = 17$). The population spike was superimposed on the slower fEPSP (Figs. 1*D* and 2*C*). As described in METHODS, the high-intensity stimulus response (dark trace) at each depth was fitted by an amplified and time-shifted response evoked by a low-intensity stimulus (light trace in Fig. 1*D* and red trace in Fig. 2*C*). The difference between the high- and low-intensity traces revealed a sharp sink at 50 μm in the apical dendrites (labeled AS in Figs. 1*D*, 2*C*, and 2*F*). The latter sharp sink peaked at ~5-ms latency in Fig. 2*F* and was interpreted as an apical dendritic (AS) spike. The AS then propagated to the cell body and basal dendrites (BS in Figs. 1*D*, 2*C*, and 2*F*). The latency of the spike sink progressively increased from 100 μm to −150 μm (stratum oriens), with the largest spike sink typically in the stratum oriens (Fig. 2*F*).

In all rats studied after apical dendritic excitation, the population spike was found to start at the proximal apical dendrites, at a depth between the maximal EPSP sink and the cell body (AS at 50–100 μm in Figs. 1*D* and 2*C*). The proximal apical population spike propagated centripetally toward the cell body layer, and then the basal dendrites. In most (6 of 8) rats in which the distal apical dendritic layer was mapped, a distal (>250 μm) apical dendritic spike was observed to start at a relatively late latency (~5 ms) at the distal border of the postsynaptic sink (AS at 200–300 μm in Fig. 2*F*). The latter spike propagated centrifugally up to 300−400 μm distal from the cell body layer; the deepest extent of propagation was not revealed in the example shown in Fig. 2*F*. Late CSDs after the spike were not interpreted. In one example shown, some of the late CSDs resulting from subtracting the low- from the high-intensity responses (open arrowhead in Fig. 2, *C* and *F*) could be generated by polysynaptic apical dendritic excitation of CA1, with minor contribution by afterpotentials and inhibition (Leung 1979a,b; Roth and Leung 1995).

The generation and propagation of the apical dendritic population spike are illustrated further by the CSD spatial profiles (Fig. 3*C*). At 3.9-ms latency, the depth profiles of the two sets of CSDs, evoked at low and high intensity, were almost identical. At 4.4-ms latency (Fig. 3*C*), small differences in the

CSDs emerged, which were interpreted as early spike sinks at the proximal dendritic locations of 100–150 μm. At 4.9-ms latency, a clear dendritic spike sink was found at 50–100 μm (Fig. 3*C*), and it was accompanied by a source at >150 μm. The spike sink progressively became maximal at 0 μm (5.4-ms latency) and −50 μm (5.9- and 6.4-ms latency). A minor distal

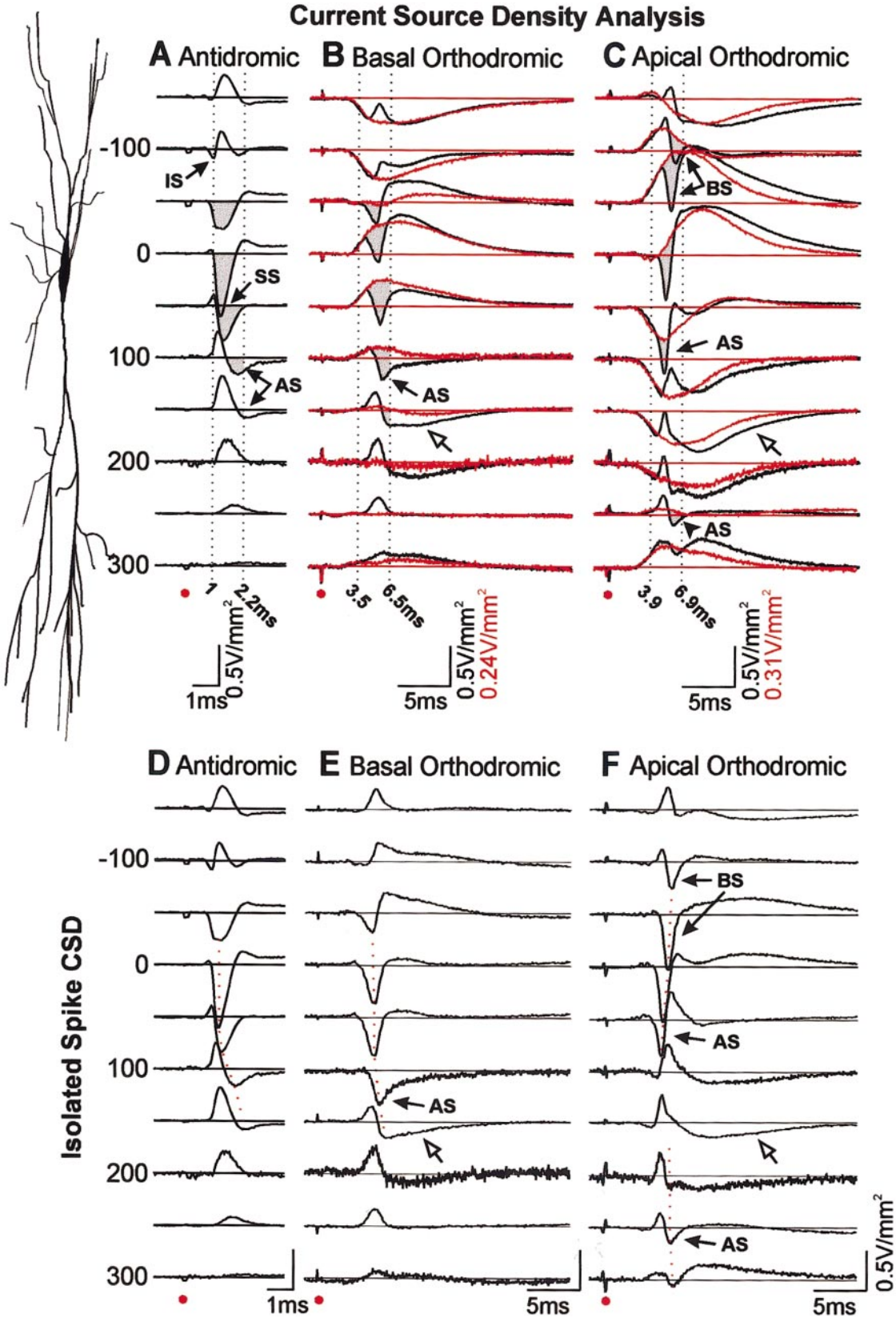

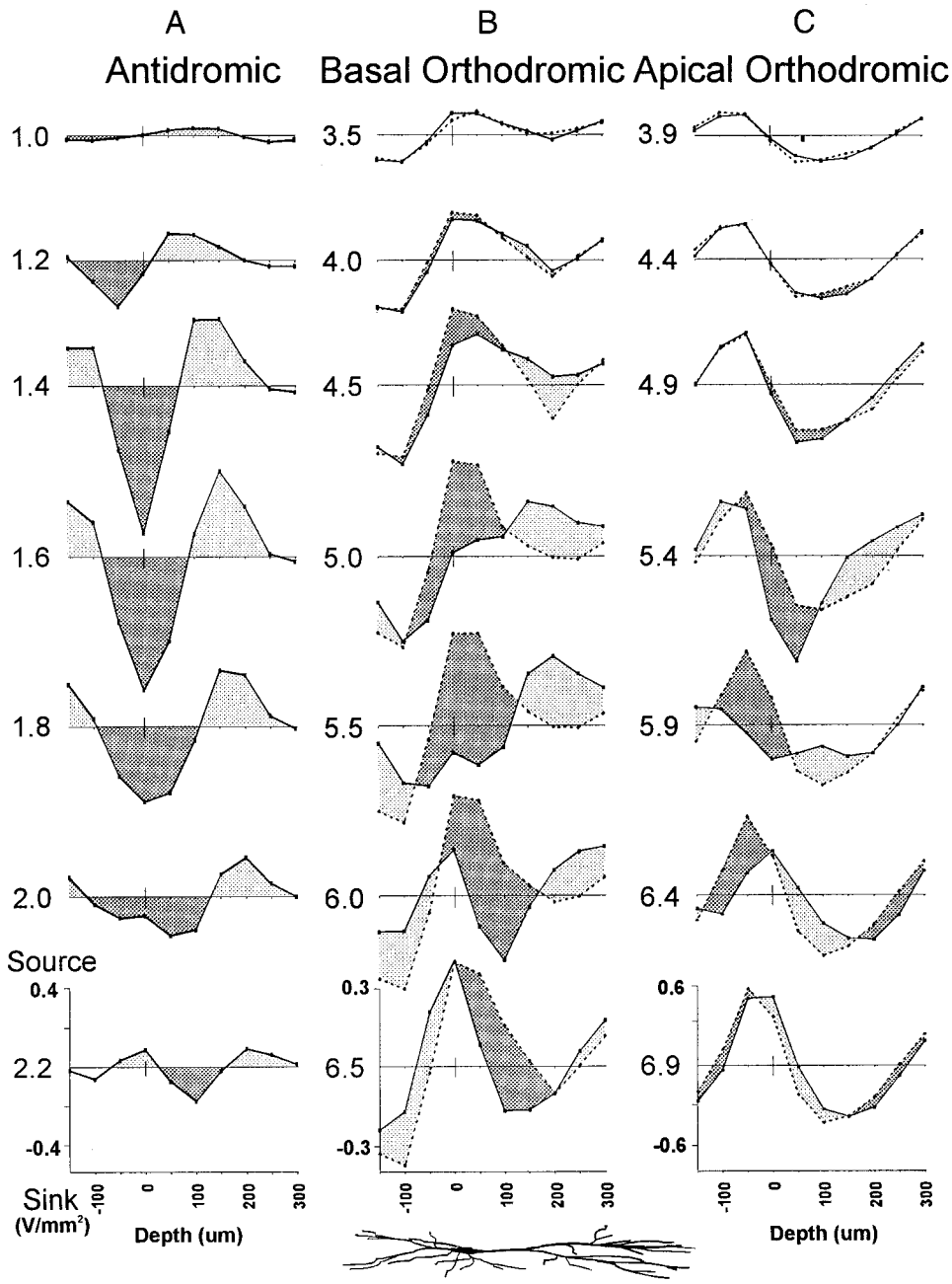

FIG. 3. CSD depth profiles at different time instants reveal an early spike sink that originates and propagates differently depending on the type of stimulation. Same CSD data of rat shown in Fig. 2. The time instants of this figure correspond to equally spaced time intervals between the vertical dotted lines in Fig. 2, *A–C*. For each plot, time is labeled in ms after stimulation on the *left*, and 0 μm (cell layer) is marked by a vertical bar. Sink (shaded dark) corresponds to the spike component evoked by high- as compared with the low-intensity (no-spike) response; source is shaded light. *A*: following antidromic stimulation, the earliest CSD pattern at 1- or 1.2-ms latency (numbers on *left* of traces) revealed a sink in stratum oriens (-100 and -50 μm). The spike sink then propagated to the cell layer at 1.4- to 1.8-ms latency, and to the apical dendrites at 2- and 2.2-ms latency. *B*: following basal dendritic excitation, the early pattern of CSDs was a stratum-oriens sink and cell-body-layer source, typical of basal dendritic fEPSPs (3.5-ms latency). Solid and dotted traces are high- and low-intensity CSDs, respectively, with low-intensity CSDs amplified and time shifted optimally to reproduce the rising fEPSP of the high-intensity CSDs. The spike sink appeared at -50 to $+50$ μm at 4-ms latency. This sink increased in magnitude (4.5- to 5.5-ms latency) and propagated toward the apical dendrites (6- to 6.5-ms latency). *C*: following apical dendritic excitation, the early pattern of CSDs was the characteristic radiatum-sink, surrounded by sources in basal dendrites and the distal apical dendrites (3.9-ms latency). The 1st spike sink appeared at 100–200 μm at between 4.4 and 4.9 ms. At 5.4 ms, the sink had propagated to the cell body, and at 5.9–6.4 ms to stratum oriens. A distal apical dendritic sink (200–300 μm) was observed at 6.4 ms as well. Spike sinks were subsiding at 6.9 ms, leaving a CSD pattern generated by fEPSPs. Schematic CA1 pyramidal cell drawn at *bottom* of *B* for depth reference.

dendritic sink also developed at 200–250 μm at 6.4- to 6.9-ms latency. The CSD profiles of the isolated population spike (resulting from subtracting the low- from the high-intensity response) are shown in Fig. 4*B*. At 4.9 and 5.4 ms, a single spike sink is surrounded by sources (Fig. 4*B*). At >5.9 ms, an additional distal dendritic spike sink is shown at 200–300 μm.

FIG. 2. CSD transients in CA1 of another rat (*PBP39*) following antidromic (*A*), basal orthodromic (*B*), or apical orthodromic stimulation (*C*). *A*: antidromic population spike was evoked by alvear stimulation of 30 μA. The antidromic spike shows the sequence of propagation from an initial segment spike (IS), a somatic spike (SS), and ended as an apical dendritic spike (AS). *B*: basal dendritic responses was evoked by 120-μA (black traces) stimulation of the stratum oriens of CA3a, overlaid on traces evoked by 50 μA stimulation, below the population spike threshold (60 μA). Basal dendritic excitation induced a spike apparently near the cell body (0 μm), and invaded the apical dendrites. Spike sink was shaded gray. Open arrowhead at 150 μm indicates deviation between high- and low-intensity responses that may be attributed to polysynaptic late excitation/inhibition or spike afterpotentials. *C*: apical dendritic responses evoked by 120 μA (black traces) stimulation of stratum radiatum of CA3b, overlaid on amplified and time-shifted responses evoked by 40-μA (red traces) stimulation. Apical dendritic excitation evoked the earliest latency spike at 50 μm, which propagated to the basal dendrites (BS). A small apical dendritic spike (arrowhead) was also apparent at 200–300 μm in the midapical dendrites. For all parts of the figure, the pair of dotted vertical lines indicated the period of time CSD depth profiles are shown in Figs. 3 and 4. *D*: same as in Fig. 2*A*, provided for alignment of *E* and *F*. *E*: the isolated CSD of the population spike following basal dendritic excitation. At each depth, the trace is the result of the black (high-intensity) minus the red (low-intensity) trace in *B*. *F*: the isolated CSD of the population spike following apical dendritic excitation, by subtracting the red trace from the black trace in *C*. CSD calibration applies to *D–F*.

CSDs following apical dendritic excitation of various stimulus intensities were studied in 10 rats. As shown in Fig. 5, *A* and *D*, a stimulus intensity of 180 μA evoked CSDs corresponding to a near-threshold population spike of amplitude ~0.3 mV (measured at −50 μm). The population spike potential increased progressively with stimulus intensity until saturation at ~350 μA (Fig. 5*F*). Irrespective of stimulus intensity, all CSD profiles show that the population spike started at the proximal apical dendrites (50–100 μm) and then propagated centripetally toward the soma and basal dendrites. The involvement of the proximal apical dendritic location of 100 μm during the onset of the population spike (*, Fig. 5) was more apparent at stimulus intensities that were above threshold (Fig. 5, *B*, *C*, and *E*) than at near-threshold (Figs. 5, *A* and *D*). However, instantaneous spatial CSD profiles (plots similar to Fig. 3; not shown) did not reveal a difference between the onset of a population spike evoked at near-threshold and suprathreshold stimulus intensities. The propagation of the spike to the basal dendrites (BS at −50 and −100 μm in Fig. 5, *A–E*) was found at all stimulus intensities, although small at near-threshold intensity (Fig. 5*D*). Fewer and more temporally dispersed unitary spikes (Andersen et al. 1971) may account for the small and wide population spike at near-threshold intensity, especially at onset and long latencies.

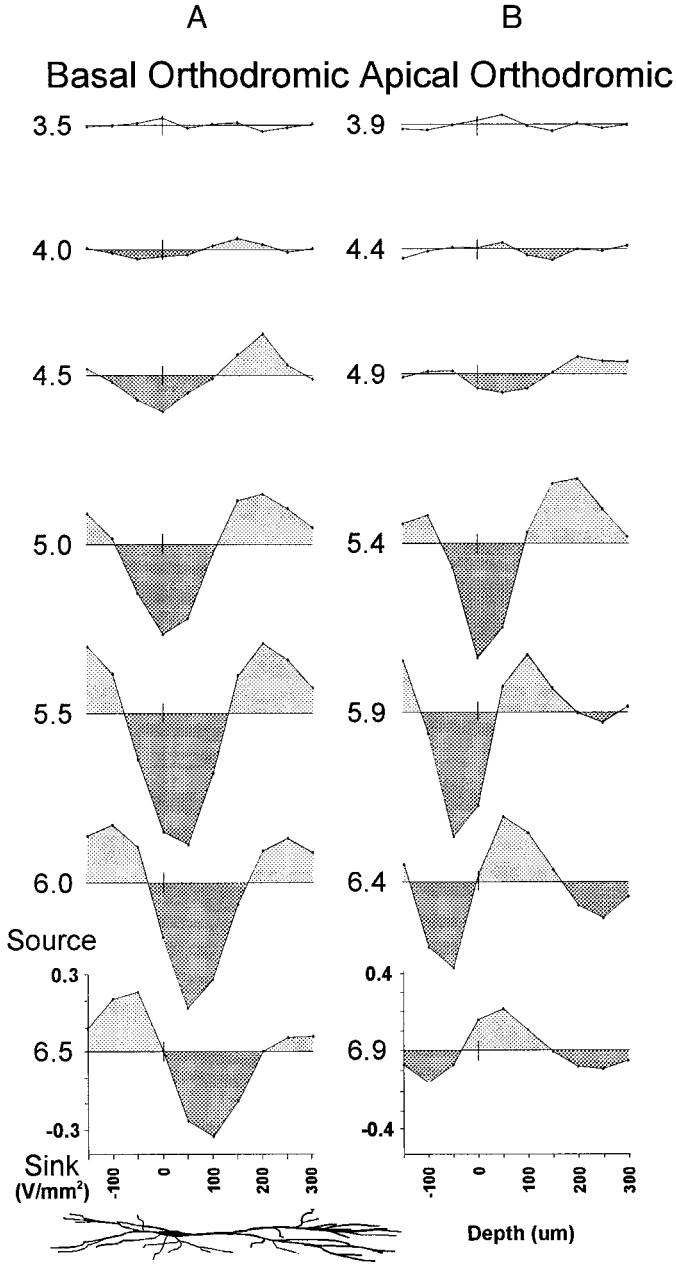

FIG. 4. CSD depth profiles at different time instants of the isolated population spike for basal dendritic excitation (*A*) and apical dendritic excitation (*B*). Data and display are similar to Fig. 3, except the isolated population spike CSD profiles are plotted. The population spike CSD at each depth was isolated by subtracting the low-intensity response from the high-intensity response.

Basal dendritic evoked population spikes starting near the cell body layer

Stimulation of CA3b stratum oriens evoked fEPSPs that were negative at the basal dendrites and positive at the cell layer and apical dendrites. The stimulus threshold for the basal fEPSPs was 30 ± 6.5 μA (n = 10). CSD analysis revealed maximal sink for the fEPSPs at stratum oriens (−100 μm in Fig. 2*A*) and maximal source at the cell layer, confirming excitation of CA1 at the basal dendrites (Roth and Leung 1995).

The stimulus threshold for a population spike following basal dendritic excitation was 119 ± 15 μA (n = 10). Again, the population spike was shown by subtracting the CSD transients following low-intensity stimulation (red traces in Fig. 2*B*) from those following high-intensity stimulation (black traces), yielding traces in Fig. 2*E*. The low- and high-intensity responses overlapped each other before the onset of the population spike, as is expected for an optimal curve fit of the fEPSP. The earliest deviation of the high- from the low-intensity stimulus-evoked CSDs occurred at about 4-ms latency, with the onset of a sink occupying −50 to 50 μm (Figs. 3*B* and 4*A*). This was interpreted as the onset of the population spike sink. Among a group of 10 rats, the earliest population spike showed a maximal sink from −50 to 50 μm, i.e., near the cell layer. In the example shown, the earliest population spike sink peaked in 4-ms latency at −50 μm, but the sink was spread over 150 μm. Within ~0.5 ms, the maximal sink shifted to 0 μm (Figs. 3*B* and 4*A*). At 5- to 6.5-ms latency, the spike sink was seen to progressively invade the proximal apical dendrites, up to about 200 μm (Figs. 2*E*, 3*B*, and 4*A*). This pattern of onset of the population spike near the soma, followed by propagation of the spike into the proximal apical dendrites, was found in all 10 rats after basal dendritic excitation. The progressive shift of a spatial pattern of "source-sink-source" to increasing depth (basal to apical direction in Fig. 4*A*) illustrates this propagation.

Latency and amplitude of peak population spike sinks

The plot of antidromic spike peak latency as a function of depth (Fig. 6*A*) reveals that the spike peak was progressively delayed from stratum oriens (−150 μm) to the proximal apical dendrites (200 μm). The conduction velocity of the peak sink from −150 to 0 μm was estimated at 0.31 ± 0.03 mm/ms (by linear regression analysis), higher than the conduction velocity in the proximal apical dendrites (from 50 to 200 μm), which was estimated at 0.14 ± 0.01 (Fig. 6*A*). The most distal

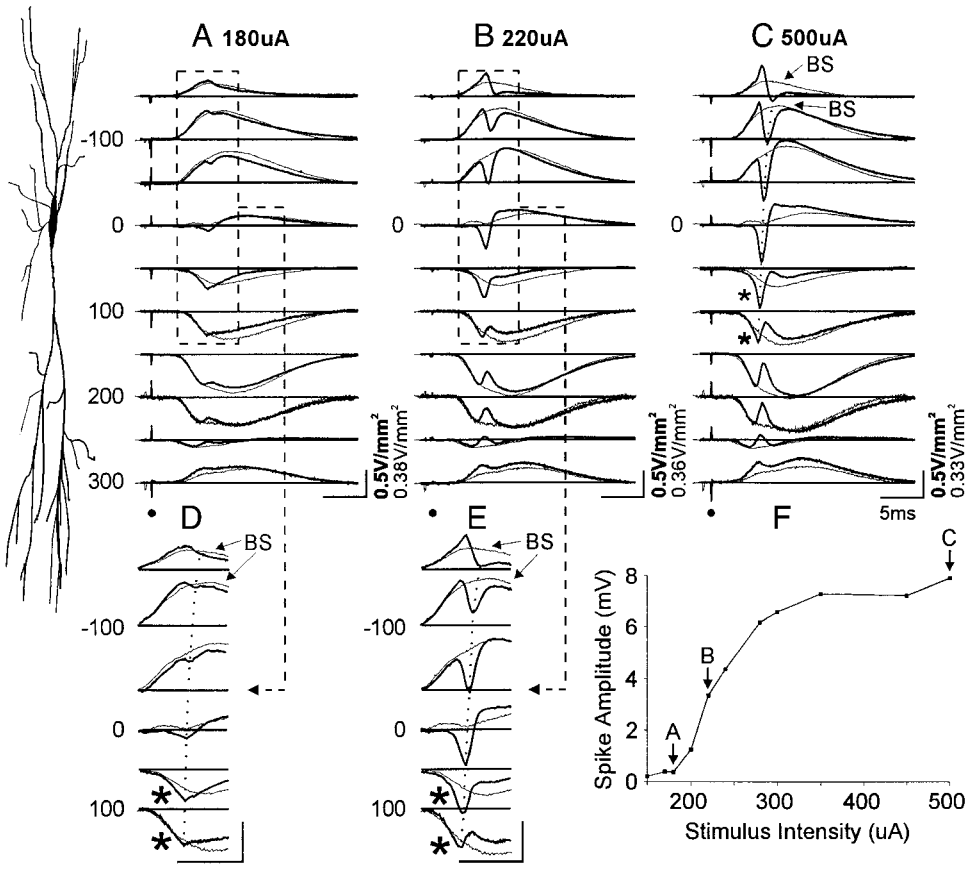

FIG. 5. CSD transients following apical orthodromic stimulation of various intensities show the same spike origin at the proximal apical dendrites. All CSDs were derived from AEPs averaged from 4 sweeps of stimulation of CA3b of intensity. *A*, 180 μA; *B*, 220 μA; and *C*, 500 μA (dark traces). Low-intensity (60 μA) CSD transients (light traces) were scaled to fit the high-intensity (dark) traces. *D*: part of *A* was expanded. *E*: part of *B* was expanded. *F*: the amplitude of the population spike in the AEPs at -50 μm (measured from onset to the negative peak) was plotted as a function of stimulus intensity, showing just-above threshold response at 180 μA and near-maximal response at >350 μA. Rat (*PBP40*) as Fig. 1; calibrations in *D* and *E*, same as *A* and *B*, respectively.

propagation of a fast antidromic spike sink was found at 157 $\pm$ 8 μm ($n = 21$; range 100–200 μm). However, the peak amplitude of the antidromic spike sink progressively decreased from 0 to 200 μm (Fig. 6*B*).

The orthodromic population spike following basal dendritic excitation shows a progressive delay similar to the antidromic spike, i.e., the delay increased from -100 to 200 μm (Fig. 2*E* and Fig. 6*A*). The average conduction velocity was 0.17 $\pm$ 0.01 mm/ms, and not statistically different between proximal basal and apical dendrites. In contrast, the delay in peak spike latency was reversed for the population spike following apical dendritic excitation. The progressive delay of the spike peak from apical to basal dendrites gave an estimate of the average conduction velocity of 0.15 $\pm$ 0.01 mm/ms (Figs. 2*F* and 6*A*).

The maximal sink of all types of population spikes peaked near the cell body layer and declined distally (Fig. 6*B*). The population spike following basal dendritic excitation tends to peak near the proximal basal dendrites (Fig. 6*B*) or the cell layer (Fig. 2*E*).

Spatial smoothing and conductivity

The CSD waveforms derived with ($n = 2$ in *Eq. 1*, METHODS) and without spatial smoothing ($n = 1$ in *Eq. 1*) are shown in Fig. 7, *A* and *B*, respectively. These CSD profiles, assuming uniform conductivity, are similar except for a difference in absolute amplitudes. The CSDs were then derived using nonuniform, layer-by-layer conductivity values (*Eq. 2*, METHODS). The main assumption was a lower conductivity at the CA1 pyramidal cell layer and the alveus, and it resulted in smaller CSD amplitudes near the soma (including the somatic spike sink; Fig. 7*C*). However, the conclusions about the onset or pattern of propagation of the population spikes remain the same with nonuniform conductivity (Fig. 7).

DISCUSSION

Different spike origins for orthodromic basal or apical spikes

One main finding of this study is that apical and basal dendritic excitation resulted in action potentials that initiated at different locations of the CA1 pyramidal cells. Basal dendritic excitation evoked a spike that started near the cell body or initial segment and then invaded the proximal apical dendrites. The latter sequence is similar to that of an antidromic spike. In contrast, apical dendritic excitation resulted in an orthodromic spike that started at the proximal apical dendrites and propagated to the cell body and basal dendrites.

The origin of the spike following apical dendritic (stratum radiatum) excitation was located at the proximal apical dendrites, 50–150 μm from the cell body. This initiation site was found following low- or high-intensity stimulation of CA3. This spike initiation site corresponds to the first- or second-order apical dendritic branches of the CA1 pyramidal cells. At the time of its onset, the spike sink was at a mid-apical-dendritic location of 100–150 μm, although relatively small in amplitude. The sink then increased severalfold in amplitude, while it invaded the more proximal dendrites (50 μm). Based on its fast time course, it may be inferred that the spike sinks were mediated by voltage-dependent Na^+ currents (Miyakawa and Kato 1986; Turner et al. 1989), and not by the long-

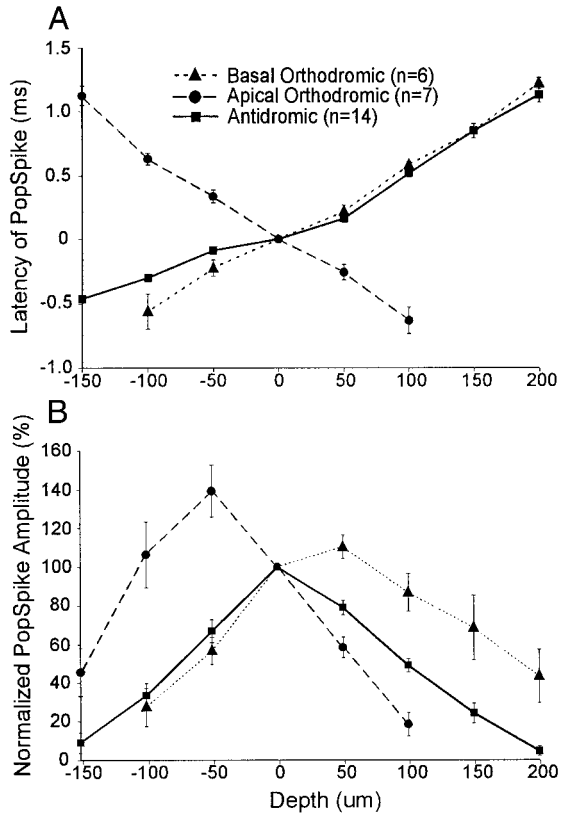

FIG. 6. Mean and SE of the peak latency and the peak amplitude of different types of population spikes as a function of depth in CA1. Error bar is ±1 SE; small error bars may be occluded by the symbols. Population spikes include antidromic, basal orthodromic, and apical orthodromic spikes. Depth is plotted as deviation from the cell body layer (0 μm). *A*: peak latency, measured as deviation from the peak latency at 0 μm, of antidromic and basal orthodromic population spike increased from stratum oriens (−100 to −150 μm) toward the mid apical dendrites (200 μm). In contrast, latency of the apical dendritic population spike increased approximately linearly from the proximal apical dendrites (100 μm) to the basal dendrites (−150 μm). *B*: peak amplitude of each type of population spike was plotted, normalized to 100% at 0 μm. The antidromic spike peaked at 0 μm (cell layer), while the basal orthodromic spike was maximal near the proximal apical dendrites (50 μm) and the apical orthodromic spike at the proximal basal dendrites (−50 μm). Only rats with clearly isolated orthodromic population spikes (see curve-fit in METHODS) were selected.

duration (>5 ms) Ca^{2+} currents (see, e.g., Golding et al. 1999; Kamondi et al. 1998).

The decline in amplitude of the fast spike sink from soma to apical dendrites (Fig. 6*B*) is consistent with the decrease in amplitude of the intradendritically recorded fast spike (Kamondi et al. 1998; Magee and Johnston 1995a,b; Turner et al. 1991). The decline of the spike height in the dendrites may be primarily caused by an increase in the density of dendritic K^+ channels (Hoffman et al. 1997), since Na^+ channel density was relatively uniform through the proximal dendrites of adult animals (Magee and Johnston 1995a,b). The ratio of Na^+ to K^+ permeability may be the most important parameter that determines the amplitude of the spike sink in the dendrites (Varona et al. 2000). In addition, the small amplitude of the spike sink at its onset in the proximal apical dendrites may be due to the small diameter of the dendritic branches and the relatively large synaptic depolarization and conductance at the apical dendrites.

A voltage-sensitive prepotential may contribute to the early onset of a proximal apical dendritic sink. Spike prepotentials may be mediated by noninactivating Na^+ currents (MacVicar 1985; Turner et al. 1989), and contributed partly by a decreasing K^+ current (Storm 1988). We suggest that a slow prepotential did not generate the early AS sink because *1*) the onset of the dendritic sink was sharp and uncharacteristic of slow prepotentials, and *2*) the spike sink at the proximal apical dendrites appeared to travel proximally at 0.15 mm/ms (Fig. 6*A*), similar to the conduction velocity of a distally backpropagating antidromic population spike.

Basal dendritic excitation of CA1 pyramidal cells evoked a population spike sink that started at a depth typically ranging from −50 to +50 μm, with the sink typically maximal at the cell body layer (0 μm) at spike onset. It is possible that proximal basal and apical dendrites were involved in spike initiation. However, a distinct and independent spike sink generated only by the dendrites is not typically revealed. At the onset of the basal population spike (4 and 4.5 ms in Figs. 3*B* and 4*A*), the sink extending from −50 to +50 μm may be caused partly by proximal dendritic sinks, or by sinks at the IS and cell bodies.

The initiation of an action potential at the proximal apical dendrites, even at low stimulus intensities, appears to be at odds with the in vitro results. A low-threshold stimulus in vitro was found to initiate an action potential at the initial segment (Spruston et al. 1995; Stuart et al. 1997) or the axon (Colbert and Johnston 1996), and only high-intensity orthodromic stimulation initiated an action potential starting at the apical dendrites (Stuart et al. 1997; Turner et al. 1991, 1993). However, a stimulus that evoked a detectable orthodromic population

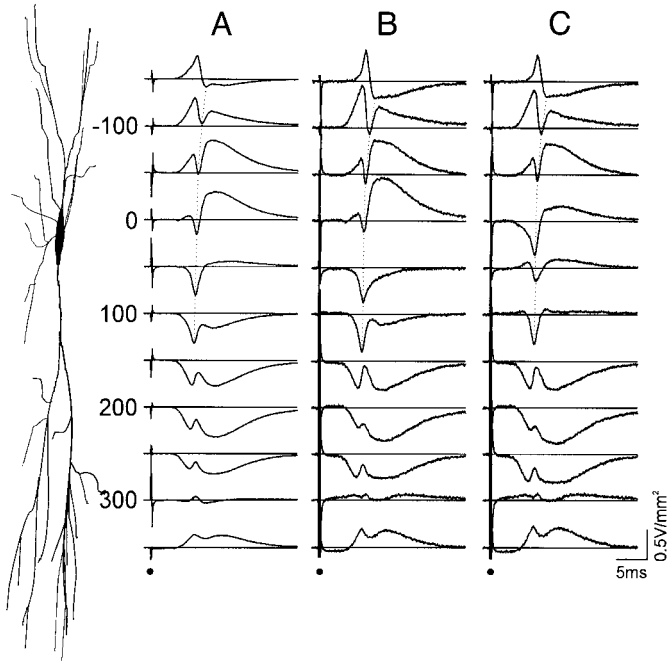

FIG. 7. CSD transients following apical orthodromic stimulation derived using different procedures. *A*: CSDs derived using a spatial interval $N\Delta z = 100$ μm ($N = 2$ in *Eq. 1*, METHODS) and uniform conductivity. *B*: CSDs derived using a spatial interval $N\Delta z = 50$ μm (*Eq. 1*). *C*: CSDs using 50-μm interval and nonuniform conductivity (*Eq. 2*, METHODS). The relative conductivities for successive 50-μm layers starting at −250 μm (alveus) were 0.8, 0.83, 0.86, 0.89, 0.93, 0.51 (cell layer), 0.75, 1, 1.05, 1.09, 1.14, 1.15, 1.15, 1.14, and 1.09 (extrapolated from Fig. 3*B* of Holsheimer 1987). The calibration applies to *A–C*.

spike in vivo (the smallest population spike was of ~0.3 mV) may be sufficiently strong to depolarize the apical dendrites and induce dendritic spiking. Even lower stimulus intensities may induce action potentials from the axon initial segments of single neurons, but these action potentials may be too temporally dispersed to result in a population spike (Andersen et al. 1971).

The origin of an orthodromic spike from the proximal apical dendrites following apical dendritic excitation confirmed the result of Herreras (1990), who used supramaximal stimulation of the CA3 region. By using simultaneous field recordings, we have extended Herreras' result to population spikes evoked by near-threshold orthodromic stimulation. Vida et al. (1995) also inferred the presence of an orthodromically evoked voltage-dependent event in the proximal dendrites in vitro, in particular after long-term potentiation. However, other CSD studies in vitro reported that the orthodromic spike originated near the cell body (Miyakawa and Kato 1986; Richardson et al. 1987). Accurate extracellular determination of the spike origin in vitro may require simultaneous recordings, which has not been done.

Herreras (1990) reported a late, proximal apical dendritic sink (LS) that was not apparent in our study, although we deliberately studied stimulus intensities near the population spike threshold. There are differences in the synaptic activation in Herreras' study and ours that may account for the presence of LS. Our CA3 stimulation typically evoked a maximal stratum radiatum synaptic sink at 200 μm, accompanied by a smooth spatial decay of the passive source that was contiguous with the synaptic sink. In contrast, Herreras (1990) evoked a synaptic sink at 100 μm that was spatially separated from a passive soma source. Although a noninactivating Na^+ current (Turner et al. 1989) may contribute to the slow LS (and initiation of a fast spike), we would also suggest a contribution by synaptic currents at the proximal dendrites.

Pattern of spike propagation

We confirmed the propagation of the antidromic spike from the inferred initial segment (stratum oriens) to the cell body. The main evidence is based on instantaneous snapshots of the CSD profiles (Fig. 3*A*) that showed a spike sink at -50 and -100 μm in the stratum oriens preceding the larger spike sink at the cell body layer (0 μm). Varona et al. (2000) inferred that a negative potential transient recorded in stratum oriens was generated by spikes at the nodes of Ranvier, but their experimental CSD data showed no stratum oriens (spike) sink preceding the somatic population spike sink.

The propagation of the antidromic population spike into the basal and apical dendrites of CA1 pyramidal cells has been shown before (Leung 1979b; Lopez-Aguado et al. 2000). Similar propagation of the orthodromic population spike into the basal dendrites has been reported in vitro (Richardson et al. 1987; Turner et al. 1989) but not in vivo. A previous in vivo study showed that the apical dendritic population spike stopped at the cell body and failed to invade the basal dendrites (Herreras 1990).

In this study, the population spike appeared to originate from the "penumbra" region of depolarization, near but removed from the site of the maximal postsynaptic depolarization. It is possible that the large synaptic sink and the passive source corresponding to the somatic spike may obscure a possible spike sink at 100–150 μm (Fig. 2*F*). We may also suggest that the mid-dendritic depolarization of pyramidal cells near the excitatory synapses is large enough to inactivate action potentials in vivo. Thus a population spike originating from the proximal apical dendrites may have difficulty traveling across the site of maximal postsynaptic depolarization, but it travels to the cell body and basal dendrites and peaked at -50 μm (Fig. 6*B*). Similarly, the population spike arising from basal dendritic excitation did not appear to invade the basal dendrites, but propagated toward the apical dendrites, where it peaked at 50 μm (Fig. 6*B*). Other factors, such as a higher ratio of voltage-dependent Na^+ to K^+ channel in the proximal than distal dendrites (Hoffman et al. 1997; Magee and Johnston 1995a,b; Varona et al. 2000) may determine spike initiation at the proximal apical dendrites, and the extent of propagation into the distal dendrites. The penumbra theory of spike onset also accounts for the late (~5-ms latency) apical dendritic spike that propagated distally from the distal border of the postsynaptic EPSP sink (AS at 250–300 μm in Fig. 2*F*).

The propagation of a dendritic spike from the apical dendrites to the basal dendrites, or vice versa, may have important functional consequences. It has been suggested that spike backpropagation may open *N*-methyl-D-aspartate or voltage-sensitive Ca^{2+} channels and thus mediate long-term potentiation (LTP) (Jaffe et al. 1992; Magee and Johnston 1995a; Stuart et al. 1997; Tsubokawa and Ross 1996). Backpropagation of the dendritic spike from one dendritic tree to the other may facilitate synaptic plasticity across basal and apical dendrites of the same CA1 pyramidal cell. Heterosynaptic LTP has indeed been observed in CA1 in vivo (Leung and Shen 1995). If a single CA1 pyramidal cell was induced to fire repetitively by basal dendritic excitation, backpropagation of the spikes to the apical dendritic synapse may induce apical LTP if there was coincident presynaptic apical dendritic afferent activity. The basal and apical dendritic trees of CA1 pyramidal cells receive inputs primarily from different sets of CA3 neurons (Ishizuka et al. 1990; Li et al. 1993). Heterosynaptic plasticity may then reinforce the functional connections from CA3 to CA1 for a small number of CA1 neurons that receive basal and apical excitation at a particular time delay.

We thank B. Shen and K. Wu for technical assistance.

This work was supported by grants from the Medical Research Council of Canada (MOP-36421) and Natural Sciences and Engineering Research Council to L. S. Leung. Silicon probes were provided by the University of Michigan, supported by National Center for Research Resources Grant P41 RR-09754. F. Kloosterman was funded by several Dutch organizations: Stichting Dr Hendrik Muller's Vaderlandsch Fonds, The Hague; Amsterdam University Society, Amsterdam; Dutch National Epilepsy Fund, Houten; Dutch Brain Foundation, The Hague; and Stichting Bekker-La Bastide-Fonds, Rotterdam.

Present address of F. Kloosterman: Swammerdam Institute for Life Sciences, Section Neurobiology, University of Amsterdam, Kruislaan 320, 1098 SM Amsterdam, The Netherlands.

REFERENCES

ANDERSEN P, BLISS TVP, AND SKREDE KK. Unit analysis of hippocampal population spikes. *Exp Brain Res* 13: 208–221, 1971.

ANDERSEN P AND LOMO T. Mode of activation of hippocampal pyramidal cells by excitatory synapses on dendrites. *Exp Brain Res* 2: 247–260, 1966.

BEMENT SL, WISE KD, ANDERSON DJ, NAJAFI K, AND DRAKE KL. Solid-state electrodes for multichaneel multiplexed intracortical neuronal recording. *IEEE Trans Biomed Eng* 33: 230–241, 1986.

BUZSÁKI G, PENTTONEN M, NÁDASDY Z, AND BRAGIN A. Pattern and inhibition-dependent invasion of pyramidal cell dendrites by fast spikes in the hippocampus in vivo. *Proc Natl Acad Sci USA* 93: 9921–9925, 1996.

COLBERT CM AND JOHNSTON D. Axonal action-potential initiation and Na^+ channel densities in the soma and axon initial segment of subicular pyramidal neurons. *J Neurosci* 16: 6676–6686, 1996.

FREEMAN JA AND NICHOLSON C. Experimental optimization of current source-density technique for Anuran cerebellum. *J Neurophysiol* 38: 369–382, 1975.

FUJITA Y AND SAKATA H. Electrophysiological properties of CA1 and CA2 apical dendrites of rabbit hippocampus. *J Neurophysiol* 25: 209–222, 1962.

GOLDING NL, JUNG H, MICKUS T, AND SPRUSTON N. Dendritic calcium spike initiation and repolarization are controlled by distinct potassium channel subtypes in CA1 pyramidal cells. *J Neurosci* 19: 8789–8798, 1999.

GOLDING NL AND SPRUSTON N. Dendritic sodium spikes are variable triggers of axonal action potentials in hippocampal CA1 pyramidal neurons. *Neuron* 21: 1189–1200, 1998.

HERRERAS O. Propagating dendritic action potential mediates synaptic transmission in CA1 pyramidal cells in situ. *J Neurophysiol* 64: 1429–1441, 1990.

HOFFMAN DA, MAGEE JC, COLBERT CM, AND JOHNSTON D. K^+ channel regulation of signal propagation in dendrites of hippocampal pyramidal neurons. *Nature* 387: 869–875, 1997.

HOLSHEIMER J. Electrical conductivity of the hippocampal CA1 layers and application to current-source-density analysis. *Exp Brain Res* 67: 402–410, 1987.

ISHIZUKA N, WEBER J, AND AMARAL DG. Organization of intrahippocampal projections originating from CA3 pyramidal cells in the rat. *J Comp Neurol* 295: 580–623, 1990.

JAFFE DB, JOHNSTON D, LASSER-ROSS N, LISMAN JE, MIYAKAWA H, AND ROSS WN. The spread of Na^+ spikes determines the pattern of dendritic Ca^{2+} entry into hippocampal neurons. *Nature* 357: 244–246, 1992.

KAMONDI A, ACSADY L, AND BUZSAKI G. Dendritic spikes are enhanced by cooperative network activity in the intact hippocampus. *J Neurosci* 18: 3919–3928, 1998.

LEUNG LS. Potentials evoked by alvear tract in hippocampal CA1 region of rats. I. Topographical projection, component analysis, and correlation with unit activities. *J Neurophysiol* 42: 1557–1570, 1979a.

LEUNG LS. Potentials evoked by the alvear tract in hippocampal CA1 of rats. II. Spatial field analysis. *J Neurophysiol* 42: 1571–1589, 1979b.

LEUNG LS. Field potentials in the central nervous system—recording, analysis and modeling. In: *Neurophysiological Techniques. Applications to Neural Systems. NeuroMethods*, edited by Boulton AA, Baker GB, and Vanderwolf CH. Clifton, NJ: Humana, 1990, vol. 15, p. 277–312.

LEUNG LS, KLOOSTERMAN F, WU K, AND PELOQUIN P. Orthodromic spike in hippocampal CA1 originates in the proximal apical or basal dendrites in urethane-anesthetized rats in vivo. *Neurosci Abstr* 26: 182, 2000.

LEUNG LS, ROTH L, AND CANNING K. Entorhinal inputs to the hippocampal CA1 and dentate gyrus in the rat: a current-source-density study. *J Neurophysiol* 73: 2392–2403, 1995.

LEUNG LS AND SHEN B. Long-term potentiation at the apical and basal dendritic synapses of CA1 after local stimulation in behaving rats. *J Neurophysiol* 73: 1938–1946, 1995.

LI X-G, SOMOGYI P, YLINEN A, AND BUZSAKI G. The hippocampal CA3 network: an in vivo intracellular labelling study. *J Comp Neurol* 33: 1–29, 1993.

LOPEZ-AGUADO L, IBARZ JM, AND HERRERAS O. Modulation of dendritic action currents decreases the reliability of population spikes. *J Neurophysiol* 83: 1108–1114, 2000.

MACVICAR BA. Depolarizing prepotentials are Na^+ dependent in CA1 pyramidal neurons. *Brain Res* 333: 378–381, 1985.

MAGEE JC AND JOHNSTON D. Synaptic activation of voltage-gated channels in the dendrites of hippocampal pyramidal neurons. *Science* 268: 301–304, 1995a.

MAGEE JC AND JOHNSTON D. Characterization of single voltage-dependent Na^+ and Ca^{2+} channels in the dendrites of rat CA1 pyramidal neurons. *J Neurophysiol* 74: 2220–2224, 1995b.

MIYAKAWA H AND KATO H. Active properties of dendritic membrane examined by current source density analysis in hippocampal CA1 pyramidal neurones. *Brain Res* 399: 303–309, 1986.

PLONSEY R. *Bioelectric Phenomenon.* New York: McGraw Hill, 1969.

RICHARDSON TL, TURNER RW, AND MILLER JJ. Action-potential discharge in hippocampal CA1 pyramidal neurones: current source density. *J Neurophysiol* 58: 981–996, 1987.

ROTH LR AND LEUNG LS. Difference in LTP at basal and apical dendrites of CA1 pyramidal neurons in urethane-anesthetized rats. *Brain Res* 694: 40–48, 1995.

SPENCER WA AND KANDEL ER. Cellular and integrative properties of the hippocampal pyramidal cell and the comparative electrophysiology of cortical neurons. *Int J Neurol* 6: 267–296, 1968.

SPRUSTON N, SCHILLER Y, STUART G, AND SAKMANN B. Activity-dependent action potential invasion and calcium influx into hippocampal CA1 dendrites. *Science* 268: 297–300, 1995.

STORM JF. Temporal integration by a slowly inactivacting K^+ current in hippocampal neurons. *Nature* 336: 379–381, 1988.

STUART GJ, SCHILLER J, AND SAKMANN B. Action potential initiation and propagation in rat neocortical pyramidal neurons. *J Physiol (Lond)* 505: 617–632, 1997.

TAUBE JS AND SCHWARTZKROIN PA. Mechanisms of long-term potentiation: a current-source density analysis. *J Neurosci* 8: 1645–1655, 1988.

TSUBOKAWA H AND ROSS WN. IPSPs modulate spike backpropagation and associated $[Ca^{2+}]_i$ changes in the dendrites of hippocampal CA1 pyramidal neurons. *J Neurophysiol* 76: 2896–2906, 1996.

TURNER RW, MEYERS DE, AND BARKER JL. Fast pre-potential generation in rat hippocampal CA1 pyramidal neurons. *Neuroscience* 53: 949–959, 1993.

TURNER RW, MEYERS DER, AND BARKER JL. Localization of tetrodotoxin-sensitive field potentials of CA1 pyramidal cells in the rat hippocampus. *J Neurophysiol* 62: 1375–1387, 1989.

TURNER RW, MEYERS DER, RICHARDSON TL, AND BARKER JL. The site for initiation of action potential discharge over the somatodendritic axis of rat hippocampal CA1 pyramidal neurones. *J Neurosci* 11: 2270–2280, 1991.

VARONA P, IBARZ JM, LOPEZ-AGUADO L, AND HERRERAS O. Macroscopic and subcellular factors shaping population spikes. *J Neurophysiol* 83: 2192–2208, 2000.

VIDA I, CZOPF J, AND CZÉH G. A current-source density analysis of the long-term potentiation in the hippocampus. *Brain Res* 671: 1–11, 1995.

WONG RKS, PRINCE DA, AND BASBAUM HI. Intradendritic recordings from hippocampal neurons. *Proc Natl Acad Sci USA* 76: 986–990, 1979.

YLINEN A, BRAGIN A, NADASDY Z, JANDO G, SZABO I, SIK A, AND BUZSAKI G. Sharp wave-associated high-frequency oscillation (200 Hz) in the intact hippocampus: network and intracellular mechanisms. *J Neurosci* 15: 30–46, 1995.